

1 A global perspective on the climate-driven growth synchrony of 2 neighboring trees

3 *Tejedor E^{1*}, Serrano-Notivol R², de Luis M^{3,4}, Saz MA^{3,4}, Hartl C⁵, StGeorge S⁶, Büntgen U⁷, Liebhold A^{8,9},*
4 *Vuille, M¹, Esper J⁵*

5
6 ¹Department of Atmospheric and Environmental Sciences. University at Albany (State University of New York), Albany (USA)

7 ²Estación Experimental de Aula Dei, Consejo Superior de Investigaciones Científicas (EEAD-CSIC), Zaragoza, Spain

8 ³Departamento de Geografía y Ordenación del Territorio. Universidad de Zaragoza (Spain)

9 ⁴Instituto Universitario de Ciencias Ambientales (IUCA). Universidad de Zaragoza (Spain)

10 ⁵Department of Geography. Johannes Gutenberg University. Mainz (Germany)

11 ⁶Department of Geography, Environment and Society. University of Minnesota. Minnesota (USA)

12 ⁷Department of Geography. University of Cambridge. Cambridge (UK)

13 ⁸USDA Forest Service Northern Research Station, Morgantown (USA)

14 ⁹Faculty of Forestry and Wood Sciences. Czech University of Life Sciences. Prague (Czech Republic)

15

16 **Abstract**

17 **Aim**

18 Previous work demonstrated the global variability of synchrony in tree-growth within
19 populations, i.e. the covariance of the year-to-year variability in growth of individual neighboring
20 trees. However, there is a lack of knowledge about the causes of such variability and its
21 trajectories through time. Here we examine whether climate can explain variation in within-
22 population synchrony (WPS) across space but also through time and develop models capable of
23 explaining this variation. These models can be applied to the global tree cover under current and
24 future climate change scenarios.

25

26 **Location**

27 Global.

28

29 **Time period**

30 1901-2012.

31

32 **Major taxa studied**

33 Trees.

34

35 **Methods**

36 We estimated WPS values from a global tree-ring width database consisting of annual growth
37 increment measurements from multiple trees at 3,579 sites. We employed generalized linear
38 mixed effects models to infer the drivers of WPS variability and temporal trends of global WPS.
39 We then predicted WPS values across the global extent of tree cover and finally, we applied our
40 model to predict future WPS based on the RCP 8.5 (2045-2065 period) emission scenario.

41

42 **Results**

43 Areas with the highest WPS are characterized by a combination of both high annual mean
44 temperature (>10°C) and low precipitation (< 300 mm) environments. Average WPS across all
45 temperate forests has historically decreased and will continue to decrease. Potential implications

46 of these patterns include changes in forest dynamics, such as higher tree growth and productivity
47 and an increase in carbon sequestration. In contrast, the WPS of tropical forests of Central and
48 South America will increase in the near future due to reduced annual precipitation.

49

50 **Main conclusions**

51 Climate explains WPS variability in space and time. We suggest that WPS may have value as an
52 integrative ecological measure of the level of environmental stress to which forests are
53 subjected, and therefore holds potential for diagnosing effects of global climate change on tree
54 growth.

55

56 **Keywords**

57 Synchrony, tree-ring, tree stress indicator, global

58

59 **1. Introduction**

60 **1.1. Importance of forests and population dynamics**

61 Forests are important carbon pools, characterized by a continuous exchange of CO₂ with the
62 atmosphere. Within all tropical, temperate and boreal forests, around 31% of carbon is stored in
63 biomass and 69% in soil (IPCC, 2000). What is more, in the past few decades 30% of global
64 anthropogenic CO₂ emissions have been absorbed by the world's forests (which is about the
65 same amount as is taken up by the oceans (Bellassen, 2014). Forests directly affect approximately
66 1.6 billion people worldwide regarding economic activities such as forestry, food, agricultural
67 policies or tourism (FAO, 2013). Hence, it is essential to better understand current and future
68 changes in forest dynamics and evolution. However, most of our understanding of forest
69 dynamics comes from retrospective analyses that consider how past events and stand structure
70 led to the development of the forests that we can observe and analyze today (Waring & Running,
71 2007). Here, we propose an additional approach to understand forest population dynamics by
72 analyzing the within-population synchrony (WPS) of tree growth.

73 This method relies on the assumption that the world around us is a spatially autocorrelated
74 system (Legendre, 1993). Derived from that concept is the spatial synchrony concept, which
75 refers to coincident changes in the abundance or other time-varying characteristics of
76 geographically disjunct populations (Liebhold, Koenig, & Bjørnstad, 2004). Many studies in
77 ecology have employed this concept to, for instance, investigate different ecological aspects of
78 great significance for tree growth, such as seed production or masting (Allen, Mason, Richardson,
79 & Platt, 2012; Kelly, 1994; Pearse, Koenig, & Kelly, 2016), host phenology (Dodd et al., 2008) or
80 foliage-feeding herbivores as synchronizing agents in forests (Peltonen, Liebhold, Bjorstand, &
81 Williams, 2002). In addition, the absence of spatial synchrony is generally considered key to
82 persistence in metapopulation dynamics and may be vitally important in the conservation of
83 species and disease eradication (Mikko, Veijo, Esa, & Jan, 1997; Noble, Machta, & Hastings, 2015).
84 Finally, it has also been suggested that an increase in spatial correlation could be an early-warning
85 signal before a regime shift (Dakos, van Nes, Donangelo, Fort, & Scheffer, 2010). By studying the
86 nature of such synchronous oscillations, we are taking steps to further understand the role of
87 synchrony in population dynamics. Though ecologists used to be frustrated in their efforts to
88 identify the cause of such synchrony (Liebhold, Koenig, et al., 2004), recent statistical advances
89 have made it much easier (Gouveia, Bjørnstad, & Tkadlec, 2015; Sheppard, Bell, Harrington, &

90 Reuman, 2016; Walter et al., 2017). The Moran effect (Moran, 1953), which describes how global
91 random disturbances affecting populations sharing a common density-dependent structure are
92 capable of bringing these populations into synch (Ranta, 1995), has been frequently used to
93 explain the ubiquity of spatial synchrony among populations of species belonging to various taxa
94 (Bjørnstad, Ims, & Lambin, 1999). Hence, the Moran effect is thought to be the result of universal
95 random but synchronous weather influences acting on spatially disjunct populations (Koenig,
96 1999; Mikko et al., 1997).

97 Although the synchrony concept has been widely used in dendroclimatology as a quality
98 measure of the chronology (Buras, 2017), the spatial synchrony of tree growth is an aspect that
99 remains poorly understood (Defriez & Reuman, 2017). Yet, tree-ring growth series provide long-
100 term spatial information that can indicate, for instance, release events and allow us to detect
101 synchronized regeneration caused by disturbance (Lorimer & Frelich, 1989; Sánchez-Salguero et
102 al., 2012; Zielonka et al., 2010) not only at regional scales but also at fine spatial scales (Aakala et
103 al., 2009; Carrer & Urbinati, 2001; Shimatani & Kubota, 2011). Following the spatial synchrony
104 approach, it has also been suggested that the earth's warming climate is synchronizing forest
105 growth across Eurasian regions and hence indicating early warning signals of climate change
106 impacts on forest ecosystems at subcontinental scales (Tatiana A. Shestakova et al., 2016).
107 Furthermore, Camarero, Gazol, Sangüesa-Barreda, Oliva, & Vicente-Serrano, (2015) applied the
108 synchrony concept to study early warning signals in the growth trends of declining and non-
109 declining trees and related the increase in synchrony with a rise in severe droughts. Hitherto, the
110 spatial synchrony concept in both ecology and dendrochronology has largely been applied to
111 analyze *among population synchrony* analyses rather than *within population synchrony* which we
112 consider here.

113
114 1.2. The within-population synchrony concept to study forests' population dynamics

115 The within-population synchrony (WPS) was first described by Liebhold, Sork, et al., (2004) to
116 study the synchronous production of large crops of seeds within a population (short distance <10
117 km) rather than among separate populations (as far as 1,000 km). Here we apply that approach
118 to tree-ring width series from individual (site) populations and calculate the WPS. We believe
119 that WPS can function as an integrative ecological measure of the level of environmental stress
120 to which forests are subjected, such as those arising from climate change.

121 In tree-ring research the average correlation of all ring-width series within a given stand,
122 indicated as RBAR (Wigley & Briffa, 1984), is a commonly employed measure of the covariance
123 among individual series in a chronology (Fritts, 1976). It is standard in dendrochronology to use
124 RBAR as a measure of chronology quality or signal recovery. Here, we are repurposing RBAR to
125 determine what environmental information might be recoverable from that metric and to indeed
126 document within-population synchrony (WPS) of neighboring trees. For relatively high-frequency
127 data, RBAR is unbiased and provides an accurate measure of the signal strength inherent in a
128 chronology (Briffa, 1999). The RBAR for a group of trees could, in theory, range from -1.0 to 1.0,
129 though in practice only positive values are meaningful (negatives values would indicate some sort
130 of antagonistic growth interaction). The higher the value, the stronger is the underlying common
131 signal; hence the lower the variance within each series, the weaker the noise and the lower the
132 number of series that must be averaged to reduce the noise remaining in the final mean
133 chronology to an "acceptable" level (Wigley & Briffa, 1984).

134 One of the strengths of the RBAR statistic is that it can be calculated for different time periods,
 135 and more importantly, it can be used for global comparisons of forests' growth response to
 136 climate change. St. George (2014) used the International Tree-Ring Data Bank for studying tree-
 137 ring width series of the Northern Hemisphere and indicated differences in the RBAR value among
 138 species and geographic location. In that study consistently high values were found for most sites
 139 in the North American Southwest, but also in northern Fennoscandia and the central Russian
 140 Arctic. Characteristically low values were found in tree-ring width records from European
 141 Mediterranean and sites and from the Himalayas (see Figure S1 as an example). The highest RBAR
 142 values were found in limber pine (*Pinus flexilis* E.JAMES), ponderosa pine (*Pinus ponderosa*
 143 P.LAWSON & C.LAWSON) and Douglas fir (*Pseudotsuga menziesii* (MIRBEL) FRANCO), all growing in
 144 western N. America.

145 This study further explores how WPS varies in both space and time. There is still a lack of
 146 knowledge regarding (i) the variability and change of WPS over time, (ii) the influence of the
 147 environment on WPS and (iii) the causes of geographical and temporal variation in WPS.
 148 Accordingly, in this study, we quantify WPS in tree growth from tree-ring measurements using
 149 the RBAR statistic to analyze the synchrony dynamics of tree-ring width in forests at a global scale
 150 (3,579 sites) and through time (1901-2012). We then identify spatial patterns and significant
 151 changes at these sites. Finally, we develop a model that is capable of explaining the variability in
 152 synchrony and apply it first, under current climate conditions, and then to forecast future
 153 conditions under a projected climate scenario.

154

155 Here we hypothesize that the within-population synchrony (WPS) of tree growth:

156 a) Increases as environmental conditions become more limiting (i.e., decreasing effective
 157 precipitation; Fritts, Smith, Cardis, & Budelsky, 1965). As a consequence, climate forcing will
 158 explain a large fraction of variation in synchrony within populations. Less synchronous growth
 159 would indicate a reduced importance of the general abiotic environmental factors (such as
 160 climate), and a greater influence of local abiotic and biotic factors (competition, insect
 161 outbreaks, fire, etc.).

162 b) Based upon the above relationships, both spatial and temporal variation in synchrony could,
 163 at least partially, be predictable globally and under different climate change scenarios. The
 164 possibility of having this predictive capability of WPS adds a new dimension to synchrony in
 165 tree-growth as an ecological tool, since it represents a surrogate measure of the level of
 166 environmental stress to which the populations are subjected and thus could be of
 167 extraordinary utility for the planning of forest management with ecological, economic (e.g.
 168 productivity) and mitigation (e.g. carbon sequestration) implications.

169

170 **2. Methodology**

171 **2.1. Data acquisition and treatment**

172 The International Tree Ring Databank (ITRDB, Zhao et al., 2019) is the largest archive
 173 containing digital tree-ring width measurements. As of June 2015, the ITRDB contained more
 174 than 4,000 ring-width records from all continents except Antarctica. These data are stored in the
 175 "Tucson Decadal Format" (Holmes, 1994) and besides the sample identification and ring-width
 176 measurements of the individual tree-ring series, the archive contains meta-data for each series,
 177 including tree species, as well as sampling site latitude, longitude and elevation.

178 In preparation for analysis, all available tree-ring records were downloaded, except for 245
179 records, which had to be removed due to errors detected within the data. Most frequent errors
180 consisted of unusual formats or multiple ring-width series with the same identification codes.
181 After removing erroneous data, 3,936 records were used. In addition, we selected records with
182 more than 10 samples per site and containing data within the 1901-2012 period in order to match
183 the tree-ring information with available meteorological data. The final dataset considered for the
184 study is composed of 3,579 records from both the northern and southern hemisphere. Even
185 though we are aware of the existence of additional datasets compiled by individual research
186 groups, we believe that using these 3,579 records with global coverage, should lead to robust
187 results, allowing us to identify the main characteristics of the tree-ring covariance and hence fulfil
188 the aims of this study. We selected the 1901-2012 period since monthly meteorological data are
189 available worldwide (CRU TS v.3.21.; Harris, Jones, Osborn, & Lister, 2014). Furthermore,
190 selection of this particular period facilitates the analysis of the influence of the recent global
191 warming trends on WPS variability.

192 In order to eliminate the tree age trend in radial growth and preserve only year to year
193 variability, i.e. the high-frequency signal, each of the 3,579 records were standardized using the
194 'dplR' package (Bunn, 2008) within R (R Development Team, 2018). First, each individual tree-
195 ring width series was detrended with a cubic spline with a 50 % frequency cutoff at 30 years (Cook
196 et al., 1990). Standardized series were obtained by dividing the observed values by the expected
197 values given by the spline function. Finally, we selected the residuals from a first-order
198 autoregressive modeling of the detrended measurement series. This method removes all but the
199 high-frequency variation in the series.

200

201 2.2. Measuring global within tree-growth population synchrony (WPS) and its trends

202 To explain changes in the strength of common patterns of tree growth over the selected
203 period, we calculated running WPS values using a 30-year moving window with a 29-year overlap
204 (i.e. moving up by one year at each step). WPS is calculated by the average Pearson correlation
205 of all ring-width series within a given stand (Wigley & Briffa, 1984). Because it is a running
206 correlation between series, it is a good measure of the common year-to-year variability through
207 time but is dependent upon the sample depth (Cook, Buckley, D'Arrigo, & Peterson, 2000). In this
208 case WPS values would range from 0, meaning a total absence of covariance within the tree-ring
209 width series to 1, including a total agreement of the year-to-year variability within the tree-ring
210 series.

211 To explore the temporal variability and change in WPS from 1901 to 2012 at each site, we
212 evaluated variability (standard deviation) and trends using the modified Mann-Kendall test for
213 autocorrelated data (Hamed & Ramachandra Rao, 1998) (at 95% confidence level).

214

215 2.3. Modeling the current and future synchrony of forest tree-growth

216 To explore the causes of variability in WPS values through time and within each site, we
217 employed generalized linear mixed effects models (GLME; using the R package lme4; Bates,
218 Mächler, Bolker, & Walker, 2015). Mixed models are ideally suited to settings in which the
219 individual trajectory of a particular outcome for a study over time is influenced both by factors
220 that can be assumed to be the same for many sites (e.g. the effect of climate) and by
221 characteristics that are likely to vary substantially from site to site (e.g. the Identification CODE-

222 ID- of each site or each population). Mixed models explicitly account for the correlations between
223 repeated measurements within each site (Ma, Mazumdar, & Memtsoudis, 2012; Moseley et al.,
224 2015). The WPS values observed at each site for different 30-year moving periods were
225 considered the response variable, while climatic conditions during each period were used as fixed
226 factors. We used mean annual temperature (T), total mean annual precipitation (P) and the
227 interaction between these terms at the grid point closest to each tree-ring site from the CRU TS
228 3.21 dataset (Harris et al., 2014) during the period 1901–2012. Given that WPS values range from
229 0 to 1, the quasibinomial family was used in order to describe the error distribution. Prior to
230 creating the model, we standardized the independent variables (with respect to the mean and
231 standard deviation) to ensure a compensated weight of each variable. In addition to taking into
232 account variations in the WPS at each individual site, we used the unique site identity code (ID)
233 as a random effect variable (Equation S1). We evaluated the accuracy of the models using a
234 likelihood ratio test by comparing the obtained models (full models) with the reduced models
235 where explanatory variables of interest were omitted, and only the intercept term was included
236 (null models). Next, we calculated the *p values* for the likelihood ratio tests that compared the
237 full and reduced models using the Chi square distribution.

238 Finally, to predict future values for the temperature and precipitation parameters during
239 the 2046-2065 period, we used an ensemble of multiple models for the RCP 8.5 scenario from
240 the CMIP5 project (AR5, uploaded 15th April 2014). We applied the model across global tree cover
241 to assess the potential effects on a global scale, including areas, such as those within the Tropics,
242 which are poorly covered by the ITRDB network. Global tree cover was classified according to the
243 World Wildlife Fund (WWF) definition of ecoregions (<https://www.worldwildlife.org/biomes/>)
244 (Table S1). The predictions in each pixel are made based on a common generic 'site' (same random
245 factor all across the space) with the objective of describing how the fixed factors (climate)
246 differentially influence synchrony across the world.

247

248 3. Results

249 3.1. Observed current synchrony values

250 Global forest WPS spanning the period 1901-2012 is shown in Figure 1a. According to the
251 WPS values of each site, we define five categories of forest growth synchrony (Table 1), ranging
252 from very low, absence of synchrony, to very high, meaning that growth in those sites is at near
253 to full agreement. The regions with the highest WPS values are western North America, in central
254 Asia and boreal forests in the Russian Arctic. In contrast, the lowest WPS values are found along
255 the east coast of North America, along the Mediterranean fringe in Europe in some parts of the
256 Himalayas in Asia and some sites in South America. Most of the sites (59%) show a low to
257 moderate synchrony. We also found that 17% of the sites have a very low to near-zero tree-
258 growth synchrony, whereas 24% of the sites show a very high or almost total tree-ring growth
259 synchrony. Lowest WPS values are located in North American boreal forests, while the highest
260 values correspond to sites located in the mountainous areas of Colorado, USA.

261

262 Results indicate that WPS of global forest populations has varied through time during the last
263 112 years (Figure 1b) i.e., it is a dynamic rather than a static indicator. In fact, among the studied
264 sites, 77% show a significant positive (gain) or negative (loss) trend through time (Figure 1c).
265 These changes are mostly low (78%) although a remarkable 21% of the sites are showing a

266 moderate to high variability, including shifts in the category, i.e. from high to moderate or from
267 moderate to high synchrony.

268 Overall the majority of sites exhibit a negative trend (decreasing WPS), as seen at sites located in
269 eastern North America, the Himalayas, the Alps, eastern Scandinavia, or southern South America.
270 On the other hand, some sites in the boreal forests of the Russian Arctic, in the mid-western US,
271 and western North America, show a significant positive trend (increase in WPS).

272

273 3.2. WPS determined by climate

274 By comparing our full model with a null model (Table 2) we demonstrate that the full model
275 (including the mean annual temperature and precipitation and its interaction as fixed factors)
276 has a better explanatory power (lower AIC and BIC). The WPS is positively related with mean
277 temperature, i.e. higher WPS occurs where and when temperatures are higher, and the WPS is
278 negatively related with precipitation, i.e. higher WPS is found in low precipitation environments
279 (Table 3). The interaction between annual mean temperature and precipitation also explains a
280 significant fraction of the WPS variance. WPS is higher in areas with high annual mean
281 temperature and low precipitation totals.

282 With these results, we now better understand the climate constraints of the observed WPS
283 (Figure 2). The results are robust (see Figure S3) and highlight the wide range of WPS levels of
284 the observed ITRDB forest populations. Hence, higher WPS values are found in dry environments,
285 including areas with precipitation below 400 mm, and mean annual temperature above 0°C.
286 Lower WPS values are found in sites with more than 1,000 mm of annual precipitation, although
287 they can also be found in dry but very cold environments (-20° to -10°C). Warm (>15°C) and wet
288 (>1,000 mm/year) environments, such as those in tropical forest areas show low to very low WPS.
289 Additional findings include the climate boundaries of the distribution limits of the ITRDB studied
290 sites, which range from 100 to almost 5,000 mm/year, and from -20°C to 26°C annual mean
291 temperature.

292

293 3.3. Model applications to the current and future climate

294 The GLME model is applied to the global tree cover under the current climate (Figures 3a and
295 4a), emphasizing the full range of WPS levels throughout Earth's tree cover. As expected, the
296 most limiting environments, including mean annual temperature around 30°C and mean annual
297 precipitation between 100 and 300 mm, are characterized by a higher predicted WPS. On the
298 other hand, areas with ~25°C mean annual temperature, and between 2,000 and 5,000 mm of
299 mean annual precipitation account for the lower predicted WPS levels (although results for these
300 particular areas must be treated with caution due to the reduced number of observations with
301 such climate conditions). Moderate WPS levels can be found in a wide spectrum of climates,
302 although with a similar mean annual precipitation of 300-600 mm and annual mean
303 temperatures that can range from -15°C to 25°C.

304 The GLME was applied to the future emission scenario RCP 8.5 for the 2046-2065 period,
305 yielding important projections (Figures 3b, 4b). First, WPS variability is projected to decline,
306 (there are no longer any tree species living below -20°C mean annual temperature), and
307 considering the current tree cover, the maximum annual temperature of some sites will be
308 pushed above 30°C. Most of the sites will have low to moderate WPS. In other words, those sites

309 facing a rise in temperature and an increase in precipitation will be less limited and thus decrease
310 their WPS. On the other hand, those sites exposed to a significant rise in temperature, but with
311 similar or lower precipitation amounts will be more limited and thus increase their tree-growth
312 WPS.

313 When considering only the effects of future climate change on WPS, larger changes in WPS
314 (Figures 3c, 4c) will occur in those places where precipitation totals are currently high (>2,000
315 mm/year), but precipitation is projected to decrease, whereas smaller changes are likely within
316 the low to moderate categories. An increase in tree-ring growth WPS will occur mainly in the
317 Mediterranean basin, in the tropical forest of India, and in the Amazon Basin rainforest. Northern
318 Hemisphere forests, on the other hand, and particularly the boreal forests, will experience no
319 change or a slight decrease in their WPS, due to an increase in precipitation.

320 **4. Discussion**

321 4.1. The potential of the internal synchrony of populations as an indicator of the level 322 of climatic stress

323 The WPS (or RBAR in the field of dendrochronology) in tree-ring research has been
324 traditionally used to define reconstruction periods (Buras, 2017) as a parameter in the Expressed
325 Population Signal (EPS) formula (Wigley & Briffa, 1984).

326 In this study, however, we used the WPS to calculate the synchrony between trees within
327 populations to study the impact of climate change in time and space on forest growth dynamics.
328 The analysis was focused on the high-frequency domain through a robust detrending.
329 Consequently, the results were not biased or affected by trend distortions that may potentially
330 occur if low-frequency detrending methods would have been applied (Melvin & Briffa, 2008). We
331 demonstrated that the WPS has a great potential to assess associated levels of climatic stress.
332 We thus encourage the use of the unbiased (retaining only the high-frequency variability) WPS
333 (or synchrony, when applied to dendroecological aspects) as a useful indicator for describing
334 forests environmental stress. In the near future, as the climate warms, it is likely that additional
335 non-synchronous endogenous disturbances such as nutrient availability, fire, permafrost melting,
336 insect outbreaks, or species-specific imprints would become increasingly dominant as factors
337 influencing tree growth, including a reduction of the effect of cold limitation (Fajardo & McIntire,
338 2012; Ponocná et al., 2018). Consequently, it is crucial to understand the current factors limiting
339 productivity of forests to better predict changes in future forests population distributions.

340

341 4.2. WPS tested on a global tree-ring dataset; opportunities and limitations

342 The WPS concept is tested with global tree-ring data from the ITRDB (3,579 single sites),
343 which is a robust and diverse dataset useful not only for dendroclimatic studies but also to assess
344 global dendroecological questions (Babst et al., 2019; St. George, 2014). The ITRDB does not
345 contain metadata on the distance between sampled trees or within forests (information that
346 could potentially alter our analysis, Figure S2). However, it is very unlikely that there is a
347 systematic trend or bias in the inter-distance between trees in the ITRDB. Since the ITRDB was
348 created, its main purpose was to develop climatic reconstructions (Zhao et al., 2019). This implies
349 that the selection of the trees to be sampled is based on maximizing the climatic signal and not
350 on other factors (such as competition, etc.). The distance between sampled trees is not explicit,
351 precisely because it is considered a variable that has no effect on growth (it is large enough).
352 Nonetheless, Zhao et al. (2019) concluded that the extensive data and coverage of the ITRDB

353 show great promise to address macroecological questions. The majority of the sites included in
354 the ITRDB correspond to the Northern Hemisphere, whose species, distributions and ecoregions
355 are well represented. On the other hand, large areas of Africa and tropical South America are
356 clearly underrepresented, especially the tropical and subtropical moist broadleaf forests, and
357 thus the results in those regions must be treated with caution. However, in this study we
358 attempted to demonstrate a global pattern of synchrony change and trend throughout the
359 twentieth century and towards the mid-late twenty-first century, being aware that the predictive
360 skills for large areas over the tropics are lower than for the temperate regions.

361 The mixed model for explaining synchrony, using data on temperature and precipitation from
362 each site, provides reliability to extend results toward areas where chronologies are largely
363 absent but potentially play key roles in the global carbon cycle or forest biomass productivity
364 (among other functions). Under the current climate, drivers of tree-ring growth have already
365 changed and will continue changing in a projected future warmer climate (Babst et al., 2019). In
366 the twentieth century the main drivers have transitioned from energy limitation toward water
367 limitation drivers, especially in the boreal and temperate zones (Babst et al., 2019), and in the
368 near future these drivers will affect growth rates of forest ecosystems (Charney et al., 2016; Tei
369 et al., 2017) and thus their internal synchrony (WPS).

370

371 4.3. Forest growth limitations associated with different factors

372 Our results show that a large proportion of the spatial and temporal variation in WPS is due
373 to the influence of climate, suggesting that the Moran effect might cause synchrony in tree-ring
374 width series also at local scales. It is well-known that weather is generally the only environmental
375 driver likely to act in the same range in space and time (Fritts, 1976). Thus, the primary factors
376 limiting tree-ring growth in forest populations are generally climatic. If climate is found to be the
377 main driver, hence the most limiting factor, it will manifest itself through synchronous growth in
378 the population. In addition, there are other global drivers, aside from climate, capable of altering
379 the synchrony, such as an increase of the atmospheric CO₂ concentration (McMahon, Parker, &
380 Miller, 2010) or a decrease in solar radiation caused by anthropogenic aerosol emissions after
381 1950 (global dimming, Liepert, 2002). On the other hand, when climatic conditions are more
382 favorable, local characteristics become more determinant for tree growth and the common
383 variance between tree-ring traits due to macroclimate is reduced (Fritts, 1976).

384

385 Our results not only support such a theory but also confirm our first hypothesis and initial
386 objective; spatial patterns of WPS are closely related to climate distribution patterns. Higher WPS
387 is found in warm and dry areas (>10°C annual mean temperature and <300 mm annual
388 precipitation) whereas a lower WPS is found in warm (mean annual temperature >15°C) and wet
389 environments (precipitation >1,000 mm/year), and in extreme cold and dry environments (mean
390 annual temperature <-10°C). Thus, the drivers that are associated with WPS are also likely drivers
391 determining the extent of forest cover. These patterns are similar to those described by Babst et
392 al., (2019). Although their results are based on growth patterns, our higher WPS zones coincide
393 with their lower growth zones and vice versa. Hence, these results also confirm our second
394 hypothesis and second goal; WPS spatio-temporal distribution patterns are closely related to
395 climate and therefore predictable (from the ITRDB database - unbiased and representative (Babst
396 et al., 2019)) at the level of global forest extent. We show that WPS is not static over time, but

397 its variation is associated with climate variability and change. This finding represents an
398 important milestone since it allows us to predict the future behavior and climatic stress levels in
399 environments where no information is available, but which may be able to sustain forest cover
400 in the future. We are thus able to detect hot spots, highlighting populations or locations that are
401 particularly sensitive to climate change, which might require focus for conservation and
402 management efforts. (Post et al., 2009). In addition, we now have the possibility of predicting
403 spatially explicit climate stress levels (WPS) in future climate scenarios which allow us to
404 determine potential adaptation/mitigation measures for specific regions.

405

406 4.4. Implications of our findings

407 Our most significant results of the spatial distribution of future WPS changes (Fig.4c) are
408 based on the most extreme projected future scenario (RCP 8.5, Riahi, Grübler, & Nakicenovic,
409 2007). This RCP is characterized by a sustained increase in greenhouse gas emissions over time,
410 leading to high greenhouse gas concentration levels (Riahi et al., 2007, 2011), including a rise in
411 global temperature of 4.9°C by 2100. While the projected temperature increase is relatively
412 spatially homogenous, the projected precipitation change varies strongly in space. Temperate
413 forests and the tropical forests of Africa and Asia are projected to experience an increase in
414 precipitation, while Mediterranean Forests and the Amazon tropical forest will be exposed to a
415 decrease ranging from 500 to 1000 mm per year (International Monetary Fund, 2017). Larger
416 changes in WPS are in agreement with projected precipitation changes (although the results for
417 the tropical areas must be treated with caution). A pronounced decrease in synchrony is
418 projected for the Northwest coast of Alaska, the Colombian, Ecuadorian and Peruvian Andes, and
419 the 'Gran Chaco' region between Paraguay and Argentina. These regions are projected to
420 experience a reduction of the thermal limitations due to rising temperature and increasing
421 precipitation, that can be interpreted as reduced climatic stress. Such a decrease of the WPS
422 would be reflected as an increase in tree-ring growth, as suggested already from some regions of
423 the globe for certain specific species (e.g. high-elevation bristlecone pines, Western N. America,
424 (Salzer, Hughes, Bunn, & Kipfmüller, 2009), boreal Eurasian forests (Shestakova, Gutiérrez,
425 Valeriano, Lapshina, & Voltas, 2019). The Mesoamerican region and the Amazon basin on the
426 other hand, will be areas with a potential increase of limiting factors, due to a reduction in
427 precipitation and an increase in temperature, leading to an enhanced climatic stress. It must be
428 mentioned that here we do not specifically account for extreme weather events, such as a higher
429 frequency of droughts or floods, nor are we considering other disturbance factors, such as insect
430 outbreaks, tree disease epidemics, or fires whose regimes may be altered with climate change.
431 In any case, based on our results, it is very likely that an increase in the WPS and therefore the
432 climatic stress in the Amazon forest will occur.

433

434 Whether tree-ring growth is positively related with carbon sequestration has been a
435 recent recurring topic (see Körner, 2006 and references therein), and the discussion is still on-
436 going. Here, we assume that CO₂ sequestration tracks tree-ring growth variability (as
437 demonstrated by (Dawes, Zweifel, Dawes, Rixen, & Hagedorn, 2014, among others). However,
438 the vast majority of species dominating the current biosphere evolved under CO₂ concentrations
439 of c.240 ppm according to ice core data considering the last 650.000 years (Körner, 2006). Thus,
440 the anthropogenic rate of atmospheric CO₂ enrichment is likely to create an unprecedented

441 environment for modern plant life, as by December 2019, the CO₂ concentration has already
442 exceeded 410 ppm (NOAA, 2019). On top of the increase in atmospheric CO₂, plants are dealing
443 with a rapidly changing climate, which is causing, for instance, a reduction in carbon
444 sequestration over the Amazon basin (Brienen et al., 2015). Since the WPS is calculated from the
445 tree-ring growth and explained by climate, we believe it is an additional and essential ecological
446 and integrative tool to be used when facing forests dynamics and evolution under future climate
447 change scenarios (climatic stress). This might allow us to identify potential patterns that indicate
448 changes in forest dynamics and the carbon balance of global ecosystems. In addition,
449 understanding long-term synchrony patterns of tree growth becomes highly pertinent to
450 identifying broad-scale emerging threats on forests and threshold tree responses to climate
451 change (Tatiana A Shestakova, Gutiérrez, & Voltas, 2018).

452

453 4.5. Population dynamics, evolution and distribution

454 Finally, one of the major uncertainties associated with climate-change projections is the
455 extent to which tree species will be able to disperse into their newly suitable habitats under
456 future climate change scenarios. Here, we provide evidence of the dependence of tree-growth
457 synchrony on climate, crucial to better understand current population dynamics and evolution.
458 However, future distributions will be determined not only by climate but also by a hierarchy of
459 factors such as dispersal ability, biotic interactions (i.e., competition and predation), genetic
460 adaptation, and abiotic factors (e.g., soil conditions). Also influencing future outcomes is the role
461 of humans. It is crucial to define what path greenhouse gas emissions will take over the next 10
462 to 50 years. Will we purposely or accidentally redistribute species as habitats change?

463 5. Conclusions

464 We demonstrate that climate determines WPS variations across space and also through
465 time. We use the most extreme climate scenario to address future synchrony of global tree-
466 growth in forests. As a result of the new climate state, some of the most important tropical
467 forests on Earth will increase their WPS and therefore undergo enhanced climatic stress, resulting
468 in a reduced potential to act as carbon sinks. On the other hand, temperate forest may benefit
469 from a warmer and more humid planet. Nonetheless, some level of uncertainty surrounding this
470 topic will remain, given the complex and stochastic nature of both plant migration and climate
471 change. All exercises of this type are predicated on General Circulation Models (GCMs). Thus,
472 improvements in global climate modelling will clearly have downstream effects on spatial
473 projections of biological responses to climate change. We therefore endorse the pursuit of
474 multiple modelling strategies to increase confidence in climate change projections. Ultimately,
475 we suggest that WPS may have value as an integrative ecological measure of the level of
476 environmental stress to which forests are subjected, and therefore holds potential for diagnosing
477 effects of climate change on tree growth.

478

479 Acknowledgments

480 ET and MV were partially supported by NSF-PIRE (OISE-1743738) and NSF-P2C2 (AGS-1702439).
481 RSN is funded by a “Juan de la Cierva” postdoctoral grant FJCI-2017-31595. ET, MS, RSN and MDL
482 are supported by the Government of Aragón through the “Program of research groups” (group

483 H38, “Clima, Agua, Cambio Global y Sistemas Naturales”). AL was supported by grant EVA4.0, No.
 484 CZ.02.1.01/0.0/0.0/16_019/0000803 financed by OP RDE and by the USDA Forest Service.

485

486 References

487

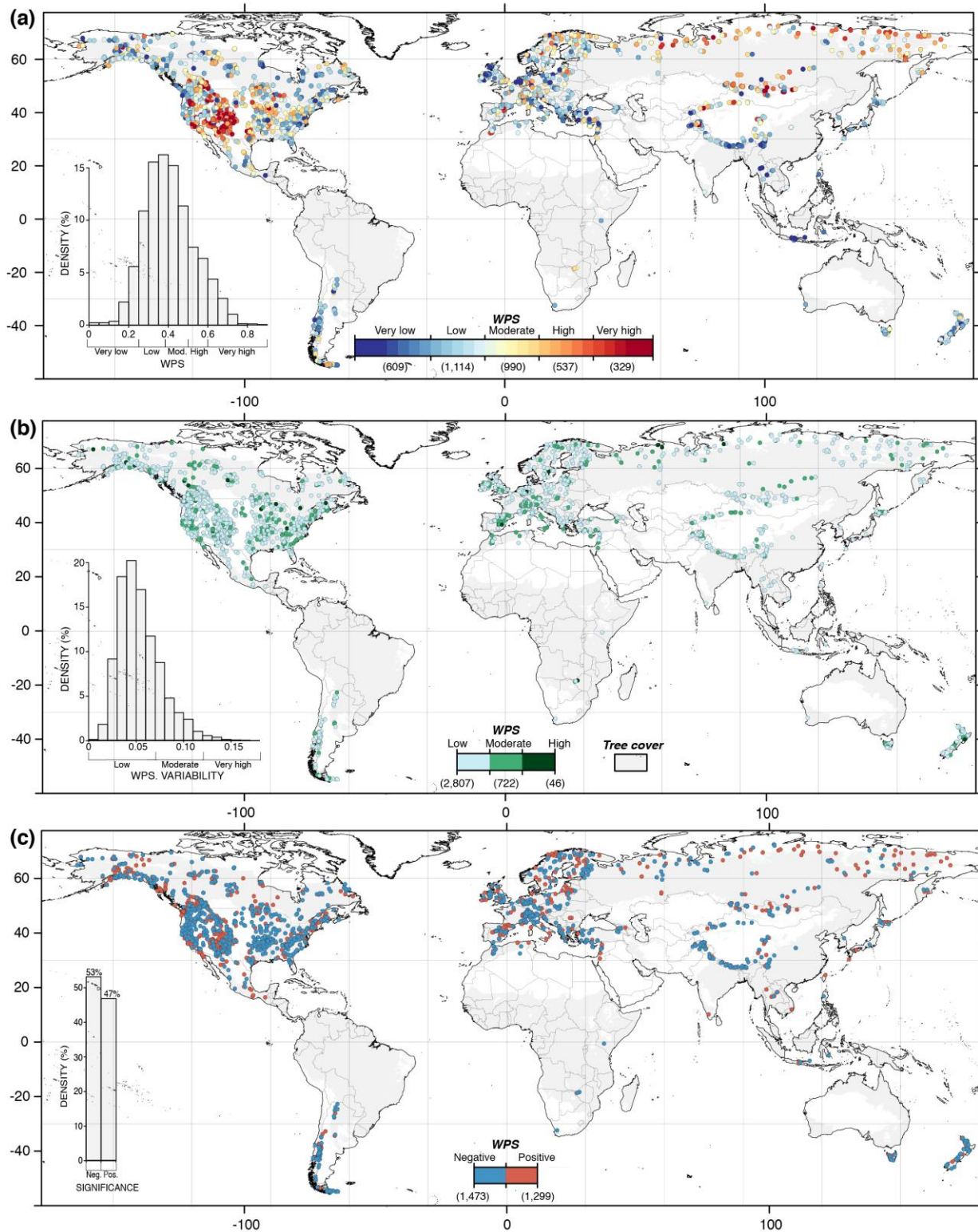
- 488 Aakala, T., Kuuluvainen, T., Wallenius, T., & Kauhanen, H. (2009). Contrasting patterns of tree mortality in late-
 489 successional *Picea abies* stands in two areas in northern Fennoscandia. *Journal of Vegetation Science*, 20(6),
 490 1016–1026. <https://doi.org/10.1111/j.1654-1103.2009.01100.x>
- 491 Allen, R. B., Mason, N. W. H., Richardson, S. J., & Platt, K. H. (2012). Synchronicity, periodicity and bimodality in
 492 inter-annual tree seed production along an elevation gradient. *Oikos*, 121(3), 367–376.
 493 <https://doi.org/10.1111/j.1600-0706.2011.19306.x>
- 494 Babst, F., Bouriaud, O., Poulter, B., Trouet, V., Girardin, M. P., & Frank, D. C. (2019). Twentieth century
 495 redistribution in climatic drivers of global tree growth. *Science Advances*, 5(1), eaat4313.
 496 <https://doi.org/10.1126/sciadv.aat4313>
- 497 Bates, D., Mächler, M., Bolker, B., & Walker, S. (2015). Fitting Linear Mixed-Effects Models Using lme4. *Journal of*
 498 *Statistical Software; Vol 1, Issue 1 (2015)* . <https://doi.org/10.18637/jss.v067.i01>
- 499 Bellassen V., L. S. (2014). Carbon sequestration: Managing forests in uncertain times. *Nature*, 506, 153–155.
 500 <https://doi.org/10.1038/506153a>
- 501 Bjørnstad, O. N., Ims, R. A., & Lambin, X. (1999). Spatial population dynamics: analyzing patterns and processes of
 502 population synchrony. *Trends in Ecology & Evolution*, 14(11), 427–432.
 503 [https://doi.org/https://doi.org/10.1016/S0169-5347\(99\)01677-8](https://doi.org/https://doi.org/10.1016/S0169-5347(99)01677-8)
- 504 Brienen, R. J. W., Phillips, O. L., Feldpausch, T. R., Gloor, E., Baker, T. R., Lloyd, J., ... Zagt, R. J. (2015). Long-term
 505 decline of the Amazon carbon sink. *Nature*, 519, 344. Retrieved from <https://doi.org/10.1038/nature14283>
- 506 Briffa, K. R. (1999). Analysis of dendrochronological variability and associated natural climates - the last 10000
 507 years (ADVANCE-10K). *PAGES Newsletter* 7 (No. 1), pp. 6–8.
- 508 Bunn, A. G. (2008). A dendrochronology program library in R (dplR). *Dendrochronologia*, 26(2), 115–124.
 509 <https://doi.org/https://doi.org/10.1016/j.dendro.2008.01.002>
- 510 Buras, A. (2017). A comment on the expressed population signal. *Dendrochronologia*, 44, 130–132.
 511 <https://doi.org/https://doi.org/10.1016/j.dendro.2017.03.005>
- 512 Camarero, J. J., Gazol, A., Sangüesa-Barreda, G., Oliva, J., & Vicente-Serrano, S. M. (2015). To die or not to die: early
 513 warnings of tree dieback in response to a severe drought. *Journal of Ecology*, 103(1), 44–57.
 514 <https://doi.org/10.1111/1365-2745.12295>
- 515 Carrer, M., Urbinati, C. (2001). Assessing climate-growth relationships: A comparative study between linear and
 516 non-linear methods. *Dendrochronologia*, 19(1), 57–65.
- 517 Charney, N. D., Babst, F., Poulter, B., Record, S., Trouet, V. M., Frank, D., ... Evans, M. E. K. (2016). Observed forest
 518 sensitivity to climate implies large changes in 21st century North American forest growth. *Ecology Letters*,
 519 19(9), 1119–1128. <https://doi.org/10.1111/ele.12650>
- 520 Cook, E. R., Buckley, B. M., D’Arrigo, R. D., & Peterson, M. J. (2000). Warm-season temperatures since 1600 BC
 521 reconstructed from Tasmanian tree rings and their relationship to large-scale sea surface temperature
 522 anomalies. *Climate Dynamics*, 16(2), 79–91. <https://doi.org/10.1007/s003820050006>
- 523 Dakos, V., van Nes, E. H., Donangelo, R., Fort, H., & Scheffer, M. (2010). Spatial correlation as leading indicator of
 524 catastrophic shifts. *Theoretical Ecology*, 3(3), 163–174. <https://doi.org/10.1007/s12080-009-0060-6>
- 525 Dawes, M. A., Zweifel, R., Dawes, N., Rixen, C., & Hagedorn, F. (2014). CO2 enrichment alters diurnal stem radius
 526 fluctuations of 36-yr-old *Larix decidua* growing at the alpine tree line. *New Phytologist*, 202(4), 1237–1248.
 527 <https://doi.org/10.1111/nph.12742>
- 528 Defriez, E. J., & Reuman, D. C. (2017). A global geography of synchrony for terrestrial vegetation. *Global Ecology*
 529 *and Biogeography*, 26(8), 878–888. <https://doi.org/10.1111/geb.12595>
- 530 Dodd, R. S., Hüberli, D., Mayer, W., Harnik, T. Y., Afzal-Rafii, Z., & Garbelotto, M. (2008). Evidence for the role of
 531 synchronicity between host phenology and pathogen activity in the distribution of sudden oak death canker
 532 disease. *New Phytologist*, 179(2), 505–514. <https://doi.org/10.1111/j.1469-8137.2008.02450.x>
- 533 Fajardo, A., & McIntire, E. J. B. (2012). Reversal of multicentury tree growth improvements and loss of synchrony at
 534 mountain tree lines point to changes in key drivers. *Journal of Ecology*, 100(3), 782–794.

- 535 <https://doi.org/10.1111/j.1365-2745.2012.01955.x>
- 536 FAO. (2013). Climate change guidelines for forest managers. In *FAO Forestry Paper No. 172*. Rome: Food and
537 Agriculture Organization of the United Nations.
- 538 Fritts, H. C. (1976). *Tree Rings and Climate* (p. 567). London: Academic Press.
- 539 Fritts, H. C., Smith, D. G., Cardis, J. W., & Budelsky, C. A. (1965). Tree-Ring Characteristics Along a Vegetation
540 Gradient in Northern Arizona. *Ecology*, 46(4), 394–401. <https://doi.org/10.2307/1934872>
- 541 Gouveia, A. R., Bjørnstad, O. N., & Tkadlec, E. (2015). Dissecting geographic variation in population synchrony using
542 the common vole in central Europe as a test bed. *Ecology and Evolution*, 6(1), 212–218.
543 <https://doi.org/10.1002/ece3.1863>
- 544 Hamed, K. H., & Ramachandra Rao, A. (1998). A modified Mann-Kendall trend test for autocorrelated data. *Journal*
545 *of Hydrology*, 204(1), 182–196. [https://doi.org/https://doi.org/10.1016/S0022-1694\(97\)00125-X](https://doi.org/https://doi.org/10.1016/S0022-1694(97)00125-X)
- 546 Harris, I., Jones, P. D., Osborn, T. J., & Lister, D. H. (2014). Updated high-resolution grids of monthly climatic
547 observations – the CRU TS3.10 Dataset. *International Journal of Climatology*, 34(3), 623–642.
548 <https://doi.org/10.1002/joc.3711>
- 549 Holmes, R. L. (1994). *Dendrochronology Program Library User's Manual*. Tucson, AZ: Laboratory of Tree-Ring
550 Research; University of Arizona.
- 551 International Monetary Fund. (2017). *World Economic Outlook, October 2017: Seeking Sustainable Growth: Short-*
552 *Term Recovery, Long-Term Challenges (World Economic and Financial Surveys)*. International Monetary
553 Fund.
- 554 IPCC, 2000. (n.d.). A Special Report of the IPCC. Land Use, Land-use Change, and Forestry. Cambridge: Cambridge
555 University Press.
- 556 Kelly, D. (1994). The evolutionary ecology of mast seeding. *Trends in Ecology & Evolution*, 9(12), 465–470.
557 [https://doi.org/https://doi.org/10.1016/0169-5347\(94\)90310-7](https://doi.org/https://doi.org/10.1016/0169-5347(94)90310-7)
- 558 Koenig, W. D. (1999). Spatial autocorrelation of ecological phenomena. *Trends in Ecology and Evolution*, 14(1), 22–
559 26. [https://doi.org/10.1016/S0169-5347\(98\)01533-X](https://doi.org/10.1016/S0169-5347(98)01533-X)
- 560 Körner, C. (2006). Plant CO₂ responses: an issue of definition, time and resource supply. *New Phytologist*, 172(3),
561 393–411. <https://doi.org/10.1111/j.1469-8137.2006.01886.x>
- 562 Legendre, P. (1993). Spatial Autocorrelation: Trouble or New Paradigm? *Ecology*, 74(6), 1659–1673.
563 <https://doi.org/10.2307/1939924>
- 564 Liebhold, A., Koenig, W. D., & Bjørnstad, O. N. (2004). Spatial Synchrony in Population Dynamics. *Annual Review of*
565 *Ecology, Evolution, and Systematics*, 35(1), 467–490.
566 <https://doi.org/10.1146/annurev.ecolsys.34.011802.132516>
- 567 Liebhold, A., Sork, V., Peltonen, M., Koenig, W., Bjørnstad, O. N., Westfall, R., ... Knops, J. M. H. (2004). Within-
568 population spatial synchrony in mast seeding of North American oaks. *Oikos*, 104(1), 156–164.
569 <https://doi.org/10.1111/j.0030-1299.2004.12722.x>
- 570 Liepert, B. G. (2002). Observed reductions of surface solar radiation at sites in the United States and worldwide
571 from 1961 to 1990. *Geophysical Research Letters*, 29(10), 61–64. <https://doi.org/10.1029/2002GL014910>
- 572 Lorimer, C.G., Frelich, L. . (1989). A methodology for estimating canopy disturbance frequency and intensity in
573 dense temperate forests. *Canadian Journal of Forest Research*, 19(5), 651–663.
574 <https://doi.org/https://doi.org/10.1139/x89-102>
- 575 Ma, Y., Mazumdar, M., & Memtsoudis, S. G. (2012). Beyond Repeated-Measures Analysis of Variance: Advanced
576 Statistical Methods for the Analysis of Longitudinal Data in Anesthesia Research. *Regional Anesthesia*
577 *& Pain Medicine*, 37(1), 99 LP – 105. <https://doi.org/10.1097/AAP.0b013e31823ebc74>
- 578 McMahon, S. M., Parker, G. G., & Miller, D. R. (2010). Evidence for a recent increase in forest growth. *Proceedings*
579 *of the National Academy of Sciences*, 107(8), 3611 LP – 3615. <https://doi.org/10.1073/pnas.0912376107>
- 580 Melvin, T. M., & Briffa, K. R. (2008). A “signal-free” approach to dendroclimatic standardisation.
581 *Dendrochronologia*, 26(2), 71–86. <https://doi.org/https://doi.org/10.1016/j.dendro.2007.12.001>
- 582 Mikko, H., Veijo, K., Esa, R., & Jan, L. (1997). Synchronous dynamics and rates of extinction in spatially structured
583 populations. *Proceedings of the Royal Society of London. Series B: Biological Sciences*, 264(1381), 481–486.
584 <https://doi.org/10.1098/rspb.1997.0069>
- 585 Moran, P. A. P. (1953). The statistical analysis of the Canadian Lynx cycle. *Australian Journal of Zoology*, 1(3), 291.
586 <https://doi.org/10.1071/ZO9530291>
- 587 Moseley, A. M., Beckenkamp, P. R., Haas, M., Herbert, R. D., Lin, C.-W. C., & Team, for the E. (2015). Rehabilitation

- 588 After Immobilization for Ankle Fracture: The EXACT Randomized Clinical Trial. *JAMA*, 314(13), 1376–1385.
 589 <https://doi.org/10.1001/jama.2015.12180>
- 590 NOAA. (2019). National Oceanic and Atmospheric Administration.
- 591 Noble, A. E., Machta, J., & Hastings, A. (2015). Emergent long-range synchronization of oscillating ecological
 592 populations without external forcing described by Ising universality. *Nature Communications*, 6, 6664.
 593 Retrieved from <https://doi.org/10.1038/ncomms7664>
- 594 Pearse, I. S., Koenig, W. D., & Kelly, D. (2016). Mechanisms of mast seeding: resources, weather, cues, and
 595 selection. *New Phytologist*, 212(3), 546–562. <https://doi.org/10.1111/nph.14114>
- 596 Peltonen, M., Liebhold, A. M., Björstand, O. N., and Williams, D. W. (2002). SPATIAL SYNCHRONY IN FOREST INSECT
 597 OUTBREAKS: ROLES OF REGIONAL STOCHASTICITY AND DISPERSAL. *Ecology*, 83(11), 3120–3129.
 598 [https://doi.org/10.1890/0012-9658\(2002\)083\[3120:SSIFIO\]2.0.CO;2](https://doi.org/10.1890/0012-9658(2002)083[3120:SSIFIO]2.0.CO;2)
- 599 Ponocná, T., Chuman, T., Rydval, M., Urban, G., Migała, K., & Treml, V. (2018). Deviations of treeline Norway
 600 spruce radial growth from summer temperatures in East-Central Europe. *Agricultural and Forest
 601 Meteorology*, 253–254, 62–70. <https://doi.org/https://doi.org/10.1016/j.agrformet.2018.02.001>
- 602 Post, E., Brodie, J., Hebblewhite, M., Anders, A. D., Maier, J. A. K., & Wilmers, C. C. (2009). Global Population
 603 Dynamics and Hot Spots of Response to Climate Change. *BioScience*, 59(6), 489–497.
 604 <https://doi.org/10.1525/bio.2009.59.6.7>
- 605 Ranta, E. (1995). Synchrony in population dynamics. *Proceedings of the Royal Society of London. Series B: Biological
 606 Sciences*, 262(1364), 113–118. <https://doi.org/10.1098/rspb.1995.0184>
- 607 Riahi, K., Grübler, A., & Nakicenovic, N. (2007). Scenarios of long-term socio-economic and environmental
 608 development under climate stabilization. *Technological Forecasting and Social Change*, 74(7), 887–935.
 609 <https://doi.org/https://doi.org/10.1016/j.techfore.2006.05.026>
- 610 Riahi, K., Rao, S., Krey, V., Cho, C., Chirkov, V., Fischer, G., ... Rafaj, P. (2011). RCP 8.5—A scenario of comparatively
 611 high greenhouse gas emissions. *Climatic Change*, 109(1), 33. <https://doi.org/10.1007/s10584-011-0149-y>
- 612 Salzer, M. W., Hughes, M. K., Bunn, A. G., & Kipfmüller, K. F. (2009). Recent unprecedented tree-ring growth in
 613 bristlecone pine at the highest elevations and possible causes. *Proceedings of the National Academy of
 614 Sciences*, 106(48), 20348 LP – 20353. <https://doi.org/10.1073/pnas.0903029106>
- 615 Sánchez-Salguero, R., Navarro-Cerrillo, R., Camarero, J. J., Fernández-Cancio, a, Swetnam, T., & Zavala, M. a.
 616 (2012). Vulnerabilidad frente a la sequía de repoblaciones de dos especies de pinos en su límite meridional
 617 en Europa. *Ecosistemas*, 21(3), 31–40. <https://doi.org/10.1175/2008MWR2773.1>
- 618 Sheppard, L. W., Bell, J. R., Harrington, R., & Reuman, D. C. (2016). Changes in large-scale climate alter spatial
 619 synchrony of aphid pests. *Nature Climate Change*, 6(6), 610–613. <https://doi.org/10.1038/nclimate2881>
- 620 Shestakova, T. A., Gutiérrez, E., Valeriano, C., Lapshina, E., & Voltas, J. (2019). Recent loss of sensitivity to summer
 621 temperature constrains tree growth synchrony among boreal Eurasian forests. *Agricultural and Forest
 622 Meteorology*, 268, 318–330. <https://doi.org/https://doi.org/10.1016/j.agrformet.2019.01.039>
- 623 Shestakova, Tatiana A., Gutiérrez, E., Kirdyanov, A. V., Camarero, J. J., Génova, M., Knorre, A. A., ... Voltas, J. (2016).
 624 Forests synchronize their growth in contrasting Eurasian regions in response to climate warming.
 625 *Proceedings of the National Academy of Sciences*, 113(3), 662–667.
 626 <https://doi.org/10.1073/pnas.1514717113>
- 627 Shestakova, Tatiana A., Gutiérrez, E., & Voltas, J. (2018). A roadmap to disentangling ecogeographical patterns of
 628 spatial synchrony in dendrosciences. *Trees*, 32(2), 359–370. <https://doi.org/10.1007/s00468-017-1653-0>
- 629 Shimatani, I. K., & Kubota, Y. (2011). The spatio-temporal forest patch dynamics inferred from the fine-scale
 630 synchronicity in growth chronology. *Journal of Vegetation Science*, 22(2), 334–345.
 631 <https://doi.org/10.1111/j.1654-1103.2010.01255.x>
- 632 St. George, S. (2014). An overview of tree-ring width records across the Northern Hemisphere. *Quaternary Science
 633 Reviews*, 95, 132–150. <https://doi.org/https://doi.org/10.1016/j.quascirev.2014.04.029>
- 634 Team, R. C. R. F. for S. C. (2018). R: A language and environment for statistical computing. Vienna, Austria.
- 635 Tei, S., Sugimoto, A., Yonenobu, H., Matsuura, Y., Osawa, A., Sato, H., ... Maximov, T. (2017). Tree-ring analysis and
 636 modeling approaches yield contrary response of circumboreal forest productivity to climate change. *Global
 637 Change Biology*, 23(12), 5179–5188. <https://doi.org/10.1111/gcb.13780>
- 638 Walter, J. A., Sheppard, L. W., Anderson, T. L., Kastens, J. H., Bjørnstad, O. N., Liebhold, A. M., & Reuman, D. C.
 639 (2017). The geography of spatial synchrony. *Ecology Letters*, 20(7), 801–814.
 640 <https://doi.org/10.1111/ele.12782>

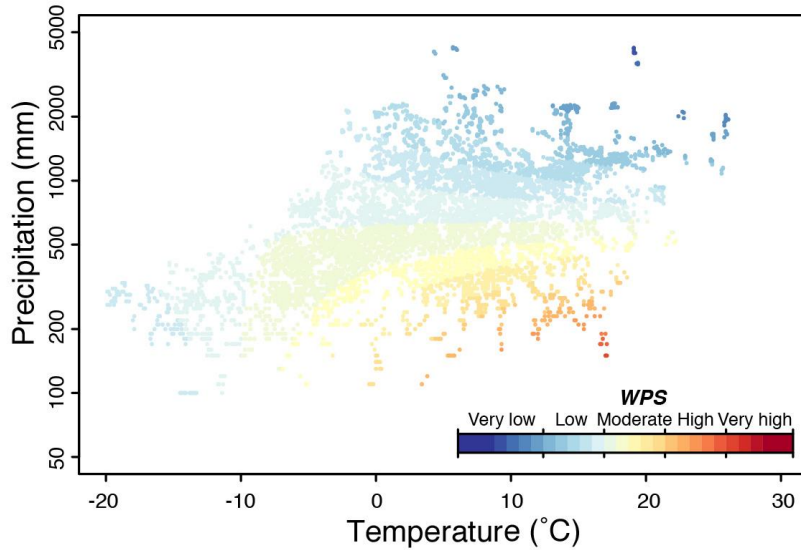
- 641 Waring, R. H., & Running, S. W. (2007). CHAPTER 1 - Forest Ecosystem Analysis at Multiple Time and Space Scales.
642 In R. H. Waring & S. W. B. T.-F. E. (Third E. Running (Eds.) (pp. 1–16). San Diego: Academic Press.
643 <https://doi.org/https://doi.org/10.1016/B978-012370605-8.50005-0>
644 Wigley TML, Briffa KR, J. P. (1984). On the average of correlated time series, with applications in dendroclimatology
645 and hydrometeorology. *Journal of Climate and Applied Meteorology*, 23, 201–203.
646 Zhao, S., Pederson, N., D’Orangeville, L., HilleRisLambers, J., Boose, E., Penone, C., ... Manzanedo, R. D. (2019). The
647 International Tree-Ring Data Bank (ITRDB) revisited: Data availability and global ecological representativity.
648 *Journal of Biogeography*, 46(2), 355–368. <https://doi.org/10.1111/jbi.13488>
649 Zielonka, T., Holeksa, J., Fleischer, P., & Kapusta, P. (2010). A tree-ring reconstruction of wind disturbances in a
650 forest of the Slovakian Tatra Mountains, Western Carpathians. *Journal of Vegetation Science*, 21(1), 31–42.
651 <https://doi.org/10.1111/j.1654-1103.2009.01121.x>
652
653
654
655
656
657
658
659

660 **Figures**

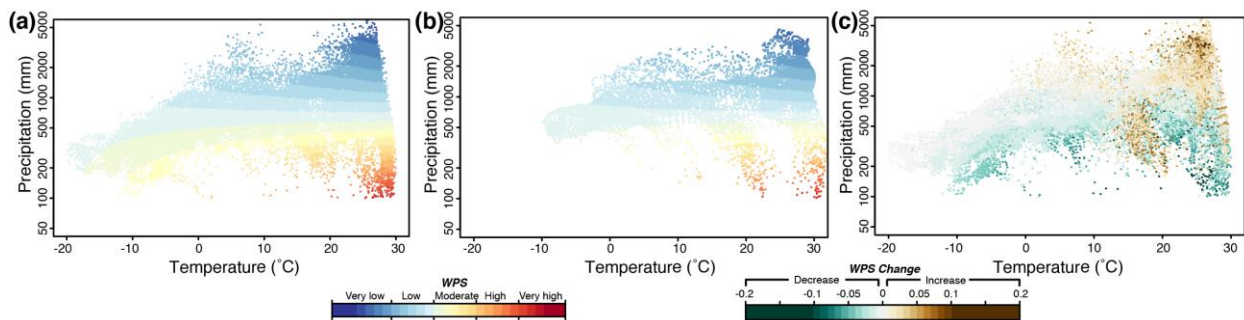


661
 662 **Figure 1.** Global patterns of within-population synchrony (WPS) at ITRDB sites for the 1901-2012
 663 period) a) Variation of WPS classified from 0 (Very Low), meaning a total absence of synchrony,
 664 to 1 (Very High), a perfect agreement between tree-ring growth series (see the categories

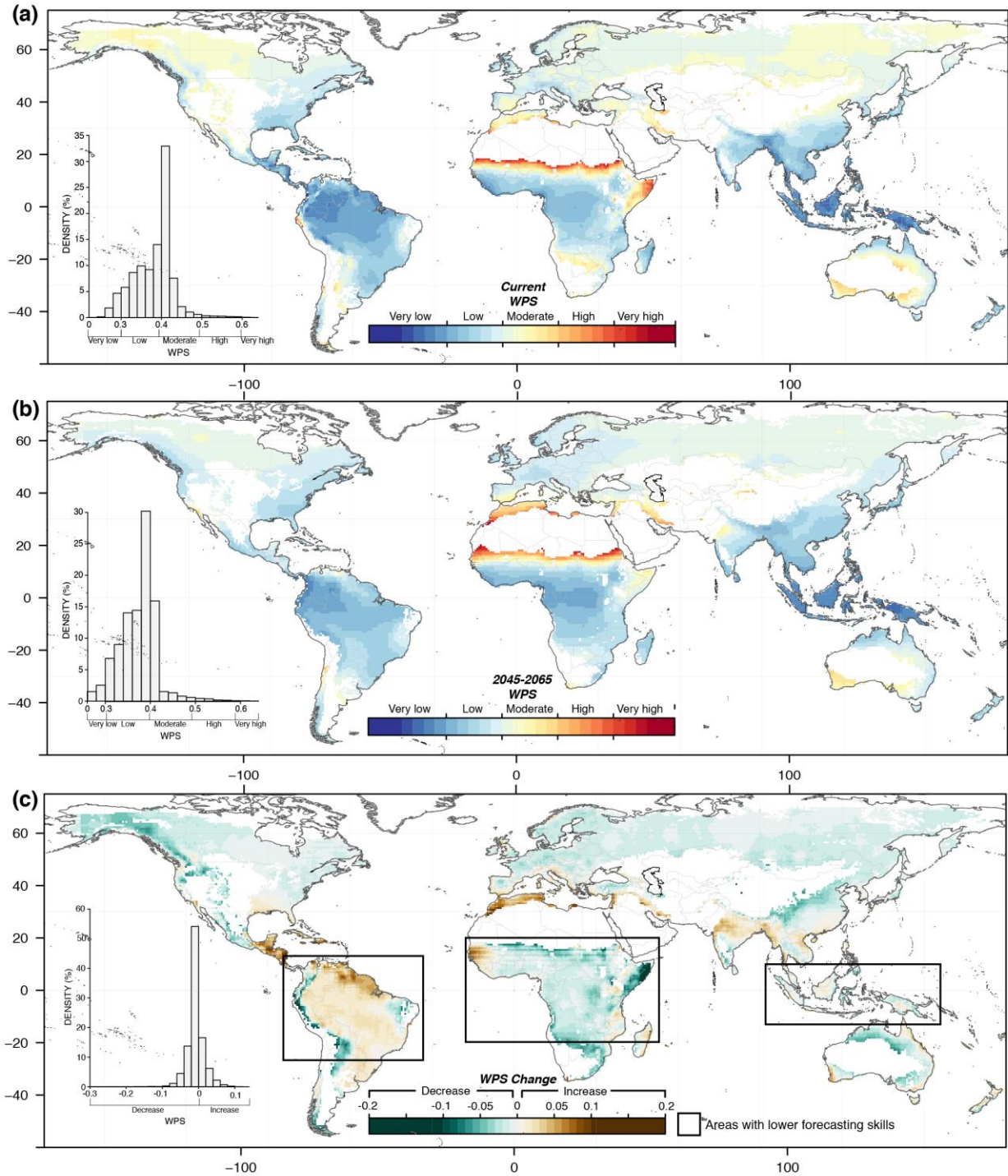
665 correspondence in Table 1) . b) WPS variability based on the standard deviation. c) Trend and
 666 significance of such WPS changes (only significance levels at $p < 0.05$ are shown).
 667
 668



669
 670 **Figure 2.** Modeled distribution of the WPS applied to the current climate (annual means) of each
 671 observed site i.e., the climate envelope covered by the tree-ring network.
 672
 673
 674



675
 676
 677 **Figure 3.** Forecasted within-population synchrony (WPS) values. a) Modeled distribution of the
 678 WPS using the current climate and applied to the global tree cover extension. b) Modeled
 679 distribution of the WPS using the RCP 8.5 scenario (2045-2065) and applied to the global tree
 680 cover extension. c) Differences in the WPS between current and future climate scenario.
 681
 682
 683



684
 685 **Figure 4.** a) Spatial distribution of the within-population synchrony (WPS) model using the current
 686 climate and applied to the global tree cover. b) Spatial distribution of the WPS model using the
 687 RCP 8.5 scenario (2045-2065) and applied to the global tree cover. c) Spatial distribution of the
 688 differences in the WPS between current and future climate scenario.

689
 690
 691

| Category | Values 1901-2012 | Change 1901-2012 |
|-----------------|-----------------------------|-----------------------------|
| Very low | < 0.30 | |
| Low | 0.30– 0.39 | <0.07 |
| Moderate | 0.40 – 0.49 | 0.07-0.12 |
| High | 0.50 – 0.59 | >0.12 |
| Very high | > 0.59 | |

Table 1. Categories of the synchrony levels.

692
693
694

| Model | Df | AIC | BIC | logLik | Deviance | Chisq | Df | Pr(>Chisq) |
|--------------|-----------|------------|------------|---------------|-----------------|--------------|-----------|----------------------|
| Null model | 2 | 224219 | 224239 | -112107 | 224215 | | | |
| Full model | 5 | 223606 | 223658 | -111798 | 223596 | 618.63 | 3 | < 2.2e-16*** |

695
696
697
698
699
700
701

Table 2. Summary statistics of the Intercept-only model (Null model) and the full model (including mean annual temperature and precipitation and its interaction as fixed factors). We include the Chi-squared test (Chisq) comparing both models. The full model has a lower AIC (Akaike information criterion) and BIC (Bayesian information criterion) than the null model indicating its better explanatory power.

| | Estimate | Std. Error | Z value | Pr(> z) |
|----------------------|-----------------|-------------------|----------------|--------------------|
| (Intercept) | 0.03550 | 0.11755 | 0.302 | 0.763 |
| TMean_Annual | 0.46642 | 0.09761 | 4.778 | 1.77e-06 *** |
| Precip_Annual | -0.14758 | 0.01797 | -0.8214 | < 2e-16 *** |
| TMean:Precip | -0.07180 | 0.01552 | -4.626 | 3.73e-06 *** |

702
703
704
705
706
707
708
709
710
711
712

Signif. codes: 0 '***' 0.001 '**' 0.01 '*'

Table 3. Full model summary of the fixed effects on the WPS. Number of observations is 186,750. WPS will be higher where temperature is higher and where precipitation is lower.

Supplementary Material

Figure S1. Example of the WPS at contrasting sites.

Figure S2. Spatial correlogram of the mean of WPS.

Figure S3. Spatial distribution of the residuals.

Table S1. Types of forests included in the tree cover.

Equation S1. Mixed model equation.